EPJ Photovoltaics **12**, 6 (2021)

https://doi.org/10.1051/epjpv/2021007

Available online at:
www.epj-pv.org

REGULAR ARTICLE OPEN ACCESS

Rear side dielectrics on interdigitating p^+-(i)-n^+ back-contact solar cells – hydrogenation vs. charge effects

Michael Rienäcker[1,*], Yevgeniya Larionova[1], Jan Krügener[2,3], Sascha Wolter[1], Rolf Brendel[1,3,4], and Robby Peibst[1,2]

[1] Institute for Solar Energy Research Hamelin (ISFH), Am Ohrberg 1, 31860 Emmerthal, Germany
[2] Institute of Electronic Materials and Devices, Leibniz Universität Hannover, Schneiderberg 32, 30167, Germany
[3] Laboratory of Nano and Quantum Engineering, Leibniz Universität Hannover, Schneiderberg 39, 30167, Germany
[4] Institute for Solid State Physics, Leibniz Universität Hannover, Appelstraße 2, 30167, Germany

Received: 1 July 2021 / Received in final form: 21 September 2021 / Accepted: 22 October 2021

Abstract. Polysilicon-on-oxide (POLO) passivating contacts and interdigitated back-contact (IBC) cell technologies have recently attracted a lot of interest as candidates for the implementation in the next generation of solar cells. An IBC cell with POLO junctions for both polarities – a POLO^2-IBC cell – has to electrically isolate the highly defective p^+ and n^+ poly-Si regions on the rear side of the cell to avoid parasitic recombination. Inserting an initially undoped, intrinsic (i) region between the p^+ and n^+ poly-Si regions was demonstrated to successfully prevent the parasitic recombination in the transition region of ISFH's 26.1%-efficient POLO^2-IBC cell. In order to further improve the conversion efficiency towards 27%, we apply hydrogen-donating dielectric layer stacks to the p^+-(i)-n^+ POLO interdigitating rear side to enhance the passivation quality of the POLO junctions. We indeed show a significant improvement of POLO junctions on symmetrical full-area homogenously doped reference samples, but when we apply a hydrogen-donating layer stack on the p^+-(i)-n^+ POLO interdigitating rear side, we observe a strong degradation in the performance of the POLO^2-IBC cell. We attribute this to the formation of a conductive channel between the p^+ and n^+ poly-Si regions due to the strong negative charge density of the hydrogen-donating layer stack.

Keywords: POLO / IBC / hydrogenation / charge / recombination / passivating contact / polysilicon

1 Introduction

The photovoltaic (PV) market demands for ever higher PV module efficiencies. Polysilicon-on-oxide (POLO) passivating contacts and interdigitated back-contact (IBC) cell technologies have recently attracted a lot of interest as candidates for the implementation in industrial production in the near future. However, the realization of an IBC cell with POLO junctions for both polarities – a POLO^2-IBC cell – requires a separation of the highly defective p^+ and n^+ poly-Si regions on the rear side of the cell to avoid parasitic recombination. Beside the trench separation [1] and local oxidation of the poly-Si [2], inserting an initially undoped, intrinsic (i) region between the p^+ and n^+ poly-Si regions – as reported by several research groups [3–6] – was demonstrated to successfully prevent the parasitic recombination in the transition region [5,7]. In 2018, a POLO^2-IBC cell with such a p^+-(i)-n^+ POLO interdigitated rear side achieved an efficiency of 26.1% [5], even without an optimized hydrogenation scheme for the POLO junctions. Thus, we recently applied hydrogen-donating layer stacks on symmetric POLO junction samples to demonstrate a significant improvement of the passivation quality compared to that implemented in the 26.1%-efficient cell from 2018 [8]. Moreover, we developed the required laser ablation process for the hydrogen-donating layer stack to be able to create laser contact openings without damaging the POLO junction underneath [9]. In this contribution, we study the interplay of hydrogen-donating layers with the p^+-(i)-n^+ POLO interdigitated rear side of our POLO^2-IBC cell. Since the typical hydrogen-donating layers like Al_2O_3 or SiN_y accommodate a high positive or negative charge, we investigate the influence of such a charge on the POLO^2-IBC cell performance. We find that any strong charge density at the p^+-(i)-n^+ POLO interdigitated rear side leads to enhanced non-ideal recombination and diminishes the performance of POLO^2-IBC solar cells.

* e-mail: rienaecker@isfh.de

2 Experimental

2.1 POLO^2-IBC solar cell precursor with different rear side dielectric layers

Figure 1a shows the structure of the precursor stage of our POLO^2-IBC solar cell fabricated similar to references [5,7]. One characteristic feature of this cell is the p^+-(i)-n^+ POLO interdigitated rear side, where the p^+-type poly-Si and n^+-type poly-Si regions are separated by an initially intrinsic (i) poly-Si region. The term "initially" refers to the fact that during high-temperature annealing, strong lateral diffusion of dopants in the poly-Si (on the length scale of several micrometres) yields an inter-diffused lateral junction [7].

In brief, the following fabrication process yielded the cell precursor in Figure 1a: A 2.2 nm-thin interfacial oxide layer was thermally grown onto a 1.3 Ωcm, p-type FZ wafer, which was subsequently capped by a low pressure chemical vapor deposited (LPCVD) intrinsic amorphous Si layer. We performed masked ion implantation of boron and phosphorous into the amorphous Si on the rear side and a blanket phosphorous implantation on the front side. For the former, the PECVD-deposited SiO_x implant mask barriers were patterned by photolithography, such that a gap of 30 µm i poly-Si remained between the n^+-type and p^+-type poly-Si fingers. Then, the amorphous Si recrystalized during a pyrogenic oxidation at 900 °C to grow a ~200-nm-thick SiO_2 layer and the POLO junction formed in a subsequent higher temperature process at 1035 °C. This step also yielded a lateral interdiffusion of dopants on the length scale of several micrometers, resulting in an inter-diffused junction within the initially 30 µm wide intrinsic poly-Si region [7]. The inter-diffused junction still isolates the charge carrier in the n^+ poly-Si from that in the p^+ poly-Si region. Hartenstein et al. have recently confirmed experimentally that the compensation of dopants at the p^+-(i)-n^+ poly-Si junction provides a highly resistive narrow region, which separates n^+ poly-Si and p^+ poly-Si electrically [10].

As in references [5,7], the POLO junctions on the rear side were hydrogenated by depositing a sacrificial hydrogen-containing, silicon-rich SiN_y layer on the thick thermal SiO_2 layer and by subsequently annealing for 30 min at 425 °C. Eventually, the SiN_y layer was removed in hot phosphoric acid.

Starting with a cell precursor as in Figure 1a, which has resulted in a cell efficiency of 26.1% in reference [3], an advanced hydrogenation scheme from Section 2.2 is applied to obtain the cell precursor in Figure 1b with improved POLO junctions on the rear side. For this purpose, we removed the SiO_2 layer from the front side and texturized it. Then, we remove the SiO_2 layer from the rear side and passivated the front side. On the rear side, we deposited a layer stack of a 20-nm-thick Al_2O_3, a 30-nm-thick hydrogen-containing silicon-rich SiN_y and a 200-nm-thick PECVD-SiO_z, which was subsequently annealed for 30 min at 425 °C.

Alternatively, we removed the layer stack from the rear side of the cell precursor in Figure 1b by a single-sided HF etching and replaced it by a 20-nm-thick PECVD-SiO_z and a 30-nm-thick SiN_y to obtain the cell precursor in Figure 1c. As indicated in Figure 1c, the 200-nm-thick SiO_z is missing on the rear side of the sample for simplicity, but has to be included in the final cell for optical reasons. The minority carrier lifetime of each cell precursor is characterized by spatially resolved infra-red lifetime mapping (ILM) [11].

Furthermore, using the same front-end process of the cell precursors in Figure 1a and b, symmetrical reference wafers with full-area doped POLO junction are fabricated and characterized by using the Sinton lifetime tester.

2.2 Advanced hydrogenation of POLO junctions

While the ~200 nm-thick thermally grown SiO_2 in Figure 1a was necessary in reference [5] to enable a damage-free local laser ablation to create contact openings, it hinders the hydrogenation of the POLO junctions from hydrogen-donating SiN_y layer to some extent. We replaced the SiO_2 by a layer stack of Al_2O_3/hydrogen-rich SiN_y/Al_2O_3, which is known to be an efficient hydrogen-donating layer stack [12] to estimate the upper limited for the passivation quality of the POLO junctions used for the 26.1%-efficient POLO^2-IBC cell. To study the effect of the improved hydrogenation scheme, symmetric p^+ POLO, n^+ POLO and iPOLO samples were prepared following the procedure in Section 2.1. After POLO junction formation, the thermally grown SiO_2 was replaced by Al_2O_3/hydrogen-rich SiN_y/Al_2O_3 and annealed at temperatures above 425 °C.

2.3 Charging of the p^+-(i)-n^+ rear side of the POLO^2-IBC solar cell precursor

In order to investigate the influence of charged dielectric layers at the p^+-(i)-n^+ rear side on the cell performance, we systematically manipulated the charge density at the rear side of cell precursor in Figure 1a and monitored the recombination behavior of the cell precursor at each charging condition. For this purpose, we deposited corona charges on top of the thermally grown SiO_2 by means of a needle-plate electrode corona discharge at 8 kV. A single charging step yielded a charge density of 4.5e11 cm^{-2}. We measured the recombination behavior of the cell precursor by using infrared lifetime mapping [11] at different illumination intensities and calculated the illumination-dependent implied open-circuit voltage Suns-i V_{OC} characteristic of the cell precursor at each charging state.

3 Results

Figure 1d shows the lifetime map of the cell wafer from Figure 1a, which contains seven cell regions (a–g) and four reference regions for iPOLO. The lifetime within the cell region b and e reach values of 1.8 ms due to the good passivation of the n^+ POLO and p^+ POLO junctions. In this stage, the full-area POLO references reveal a saturation current density of 4 fA/cm^2 and 5.5 fA/cm^2 for n^+ POLO and p^+ POLO junctions, respectively.

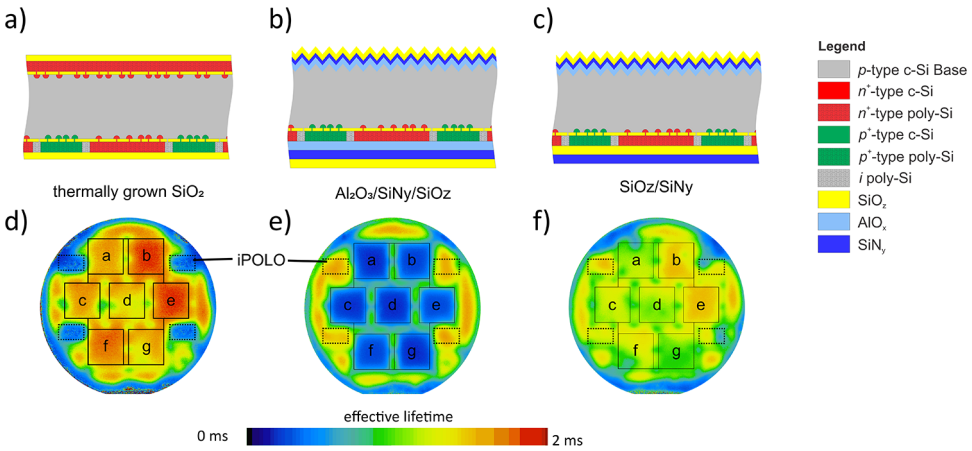

Fig. 1. (a–c) Schematic drawing of the structure of a POLO^2-IBC solar cell with (a) a thermally grown SiO_2 layer, (b) $Al_2O_3/SiN_y/SiO_z$ or (c) PECVD-SiO_z/SiN_y stack as the rear side dielectric layer. (d–f) Spatially resolved carrier lifetime of the cell structures shown in (a–c) at ∼0.25 suns measured by the ILM method. The active cell areas of the seven solar cells are marked with squares a–g.

However, as already reported in reference [7], the intrinsic reference region (*i*POLO) in Figure 1d is almost unpassivated and therefore yields low lifetimes. In contrast to that, properly hydrogenated *i*POLO junctions have been reported elsewhere [4]. This is a strong evidence that the thick SiO_2 hinders hydrogen from reaching the thin interfacial SiO_z of the *i*POLO junctions of the 26.1%-efficient cell in reference [5] and that the hydrogenation of n^+ and p^+ POLO junctions is not optimal. Thus, it seems straight forward to apply a better hydrogenation scheme to improve the POLO^2-IBC cell efficiency of 26.1% towards 27%.

Indeed, when replacing the thick SiO_2 layer by the Al_2O_3/hydrogen-rich SiN_y/Al_2O_3 layer stack and performing an annealing above 425 °C, we have been able to improve the saturation current density of our n^+ POLO and p^+ POLO junctions on symmetric lifetime samples down to below 0.5 ± 03 fA/cm^2 and 3.3 ± 0.7 fA/cm^2 [8], respectively. For the *i*POLO junction sample, an effective surface recombination velocity S_{eff} of approximately 12 cm/s is achieved after hydrogenation, which is more than an order of magnitude lower compared to the *i*POLO junction of the 26.1%-efficient cell [7]. The improved hydrogenation of the n^+ and p^+ POLO junctions from 4 fA/cm^2 and 10 fA/cm^2 to 0.5 fA/cm^2 and 3.3 fA/cm^2 was estimated to result in an efficiency improvement of ∼0.4%$_{\mathrm{abs.}}$ by means of device simulations [8].

To prove the benefit of an improved hydrogenation scheme on the cell level, we deposited a similar hydrogen-donating $Al_2O_3/SiN_y/SiO_z$ layer stack as evaluated above on the cell precursor. This results in the structure shown in Figure 1b. Figure 1e depicts the lifetime map of the cell precursor. As expected from the hydrogenation experiments above, the *i*POLO reference region of the wafer improves significantly upon hydrogenation and exhibits a lifetime of 1.5 ms. After hydrogenation, the full-area POLO references of the cell precursor in Figure 1b reveal a saturation current density of 2.5 fA/cm^2 and 4 fA/cm^2 for n^+ POLO and p^+ POLO junctions, respectively. Regardless of the improvement of the POLO junctions, the lifetime within cell regions drops from previously 1.5–1.8 ms for the cell precursor as shown in Figure 1a to about 200–300 µs for that in Figure 1b.

We explain this surprising observation by the high density of negative fixed charge in the Al_2O_3 layer in contrast to the almost neutral SiO_2 layer. The negative charge density in the dielectric layer or at its interface to poly-Si causes an upward band bending within the poly-Si layer close to its interface with the dielectric layer [13]. Thus, we expect an accumulation of holes and a depletion of electrons in the first few nm of the poly-Si layer at the Al_2O_3 interface in the degenerately doped p^+ and n^+ poly-Si region, respectively.

In the initially undoped region between the p^+ and n^+ poly-Si regions, the compensation of dopants after high temperature annealing results in a moderately doped, graded *pn* junction. In the case of an almost absent surface charge on top of the poly-Si layer e.g., with a SiO_2 layer, one part of this transition region exhibits a high resistivity and ensures electrical isolation between the p^+ and n^+ poly-Si regions. However, upon applying the Al_2O_3 layer, its strong negative fixed charge manipulates the carrier population in the moderately doped transition region, such that an accumulation and inversion layer form in the moderately doped *p*-type and *n*-type poly-Si regions, respectively. The carrier population modulation and the transport barrier lowering due to electrostatics significantly increase the carrier mobility within the poly-Si [14–18]. Thus, the Al_2O_3 effectively establishes a hole-conductive channel at its interface to the poly-Si at the p^+-(*i*)-n^+ POLO interdigitated rear side [13]. This conductive channel connects the highly defective p^+ and n^+ poly-Si regions and results in a strong recombination of electrons with holes. A similar enhanced recombination was already observed for POLO^2-IBC cells without an initially intrinsic poly-Si between p^+ and n^+ poly-Si regions [6,19,20].

In order to confirm our hypothesis, we corona charge the SiO_2 surface of the cell precursor in Figure 1a and measure the implied open circuit voltage iV_{oc} versus

illumination intensity characteristic. We systematically manipulate the charge density on the rear side by depositing a corona charge density Q_C on top of the SiO_2. First, we investigate the effect of negative charges and notice that the effect of charging the rear side on the lifetime of the precursor weakens over time. We speculate that this second order effect is due to the instability of corona charges on top of the SiO_2 layer [21,22]. On the time scale of the experiment, this instability causes an uncertainty with respect to the actual amount of charges present on the SiO_2. Qualitatively, the experiment still yields valid data. Moreover, we utilize this effect to return to the state of the cell precursor without corona charging. To reach this state, we deposit approximately the same amount of positive charges as negative charges previously applied and wait about 60 hours for the charge to neutralize. We start from this state of the precursor to study the effect of positive corona charges applied to the SiO_2.

Figure 2 summarizes the Suns-iV_{OC} characteristics for different Q_C values. If negative corona charges are deposited, the Suns-iV_{OC} curve at implied voltages close to the maximum power point of the final 26.1% cell (640 mV [5,7]) shifts towards higher illumination intensities, which corresponds to an increased non-ideal recombination with a high local ideality factor (up to 3) and which diminishes the implied pseudo fill factor. Close to one-sun conditions, the effect of charging is minor and the local ideality factor is about 0.9 for the uncharged state and 1.2 with a corona charge density of $-2.7e12\ cm^{-2}$. For positive corona charges, the Suns-iV_{OC} characteristic improves slightly up to a corona charge density of $0.9e12\ cm^{-2}$. Further increasing the positive charge densities lead again to enhanced non-ideal recombination at around a voltage of 640 mV – similar to negative charges.

Figure 3 shows the implied pseudo-efficiency iη of the cell precursor, which results from the Suns-iV_{OC} characteristic with an assumed constant short-circuit current density of $42.6\ mA/cm^2$ as has been measured for the 26.1% efficient cell in references [5,7]. Without corona charging, the cell precursor has an iη of 26.4%, which drops suddenly for negative Q_C. If a corona charge density of $0.5e12\ cm^{-2}$ or $0.9e12\ cm^{-2}$ is applied, the iη increases to about 26.5%, but drops again sharply for larger Q_C.

Given the results in Figures 2 and 3, it can be understood why the cell precursor in Figure 1b with Al_2O_3 on the rear side with a typical charge density of $-4e12\ cm^{-2}$ and the cells in reference [6] exhibits a worse recombination behavior and a compromised cell performance – even if the POLO junction's passivation quality is improved upon hydrogenation. Moreover, we expect that a cell with a strongly positively charged SiN_y hydrogen-donating layer would cause the same effect. Therefore, an IBC cell with a p^+-(i)-n^+ POLO interdigitated rear side requires an almost uncharged hydrogen-donating dielectric layer on the rear side – at least in the transition region of the p^+-(i)-n^+ junction.

Replacing the strongly charged Al_2O_3 layer by a weakly charged – optimally hydrogen-containing – PECVD/ALD-SiO_z or SiO_zN_y on the rear side of the cell precursor in

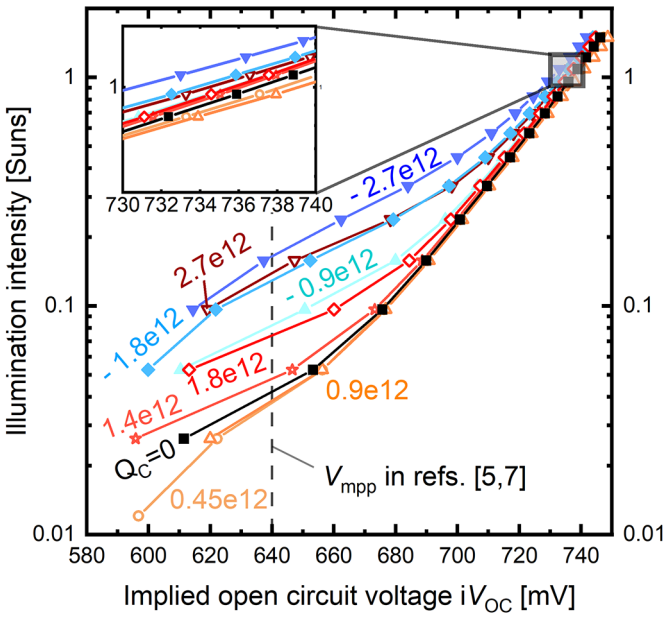

Fig. 2. Illumination-dependent implied open-circuit voltage Suns-iV_{OC} characteristic of the cell precursor from Figure 1a as a function of the applied corona charge density Q_C at the thermally grown SiO_2 on the rear side. The inset magnifies the Suns-iV_{OC} around 1 sun conditions.

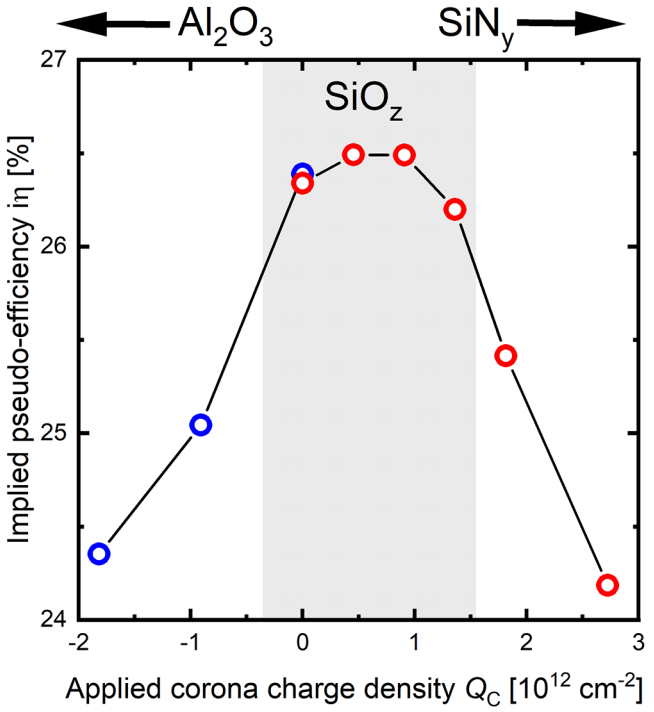

Fig. 3. Implied pseudo-efficiency iη for a cell precursor as shown in Figure 1a as a function of the applied corona charge density Q_C. Blue data points were measure first and the red ones about 60 hours after the blue data set. The arrows indicate the fixed charge density of Al_2O_3 and SiN_y on c-Si. Typical charge densities for SiO_z are marked in gray.

Figure 1b poses one possibility for such a dielectric layer stack, which could also be compatible with the laser contact opening process in reference [9].

To demonstrate that a PECVD-SiO_z meets the requirement of being weakly charged and that it is suitable for the application on the rear side of POLO^2-IBC cells, we removed the $Al_2O_3/SiN_y/SiO_z$ dielectric layer stack from a cell precursor as shown in Figure 1b and subsequently deposited a non-optimized PECVD-SiO_z and a SiN_y on the rear side. The resulting cell structure is depicted in Figure 1c. The cell precursor with a PECVD-SiO_z /SiN_y layer stack on the rear side shows a strongly improved performance in Figure 1f compared to that with an $Al_2O_3/SiN_y/SiO_z$ layer stack in Figure 1e. The cell precursors in Figure 1f exhibit an implied pseudo-efficiency of up to 26.3%. This is qualitatively comparable with the cell precursor from Figure 1d without corona charging. However, the front side passivation of the cell precursor in Figure 1a deviates from that in Figure 1c and the meaningfulness of a comparison of both cell precursors on an absolute efficiency scale is limited. However, the successful implementation of the PECVD-SiO_z on the rear side of a POLO^2-IBC cell precursor represents a good starting point for future optimization towards 27%-efficient POLO^2-IBC cells.

4 Conclusion

In this contribution, we aimed at implementing hydrogen-donating layers on the p^+-(i)-n^+ POLO interdigitated rear side to improve our POLO^2-IBC cell with an efficiency of 26.1% towards an efficiency of 27%. Since the typical hydrogen-donating layers like Al_2O_3 or SiN_y accommodate a high positive or negative charge, we investigated the influence of such a charge on the POLO^2-IBC cell performance. We fabricated POLO^2-IBC cell precursor with three different dielectric layers/layer stacks on the rear side: (i) a thermally grown SiO_2 as has been used for the 26.1% cell; (ii) a hydrogen-donating $Al_2O_3/SiN_y/SiO_z$ stack to improve POLO junction passivation quality; (iii) a hydrogen-donating PECVD-SiO_z/SiN_y stack. The implied pseudo-efficiency iη of each precursor was deduced from the illumination-dependent implied open-circuit voltage Suns-iV_{OC} of the cell precursor.

While the cell with thermally grown SiO_2 showed the expected iη of 26.4%, a comparison with the second cell precursor indicated that the hydrogenation scheme with the thick SiO_2 is less efficient compared to the $Al_2O_3/SiN_y/SiO_z$ stack. The second cell precursor with $Al_2O_3/SiN_y/SiO_z$ stack efficiently hydrogenated the POLO junction, but yielded a cell precursor with worse recombination behavior and low performance. We attributed this surprising observation to the presence of a strong negative charge induced by the Al_2O_3 layer.

To confirm this hypothesis, we studied the influence of charges at the p^+-(i)-n^+ POLO interdigitated rear side on the POLO^2-IBC cell performance. We systematically manipulated the charge density by depositing a corona charge density on top of the SiO_2 covering the rear side. We found that strong positive or negative charge densities cause an enhanced non-ideal recombination and degrade the cell performance significantly, which is most likely due to the formation of a conductive path for electrons or holes within the highly defective poly-Si. Fortunately, the thermally grown SiO_2 has a nearly ideal charge density and its iη can only slightly be improved by $0.1\%_{abs}$ to 26.5% by adding a positive corona charge density of below 0.9e12 cm^{-2}.

We conclude that it is vital to control the charge density of the dielectric layers applied to the p^+-(i)-n^+ POLO interdigitated rear side to avoid a strong increase of non-ideal recombination at the p^+-(i)-n^+ poly-Si junction. While this effect is highly pronounced for IBC cells with poly-Si, it may also apply − to some extend − to all types of IBC cells with charged dielectric layers on the interdigitated rear side.

Finally, we presented a weakly charged hydrogen-donating layer stack comprising a 20-nm-thin and a potentially weakly charged PECVD-SiO_z at the interface with the poly-Si capped by a hydrogen-donating SiN_y layer. This stack may provide an efficient hydrogenation scheme, while maintaining the isolation between p^+ and n^+ poly-Si regions. A first cell precursor with the weakly charged hydrogen-donating layer stack yielded an iη of 26.3%.

The authors thank the state of lower Saxony and the Federal Ministry of Economic Affairs (BMWi) for funding this work, which was performed in the framework of the research project "27Plus6" (FKZ03EE1056A). We are grateful to Hilke Fischer, Sarah Spätlich and Renate Winter (all from ISFH) as well as Raymond Zieseniss and Guido Glowatzki (both from Institute of Electronic Materials and Devices) for sample processing. We thank Felix Haase and Christina Hollemann for fruitful discussions.

Author contribution statement

M. R., Y. L., S. W. and R. P. designed the investigations of the improved hydrogenation and discussed the results. Y. L. supervised the experiments with respect to the improved hydrogenation, acquired and analyzed the data. M. R., J. K. and R. P. supervised the processing of the solar cell precursors. M. R. designed the corona charging experiments, collected and analyzed the data, and wrote the original draft. R. P. and R. B. supported the POLO work at ISFH with many fruitful discussions, corrected the manuscript and acquired the financial support. All authors discussed the results and revised the manuscript.

References

1. D. De Ceuster, P.J. Cousins, D.D. Smith, Trench process and structure for backside contact solar cells with polysilicon doped regions, Patent US Patent 7,851,698, 2010
2. U.R. Robby Peibst, Solar cell and a method for producing a solar cell with oxidised intermediate regions between polysilicon contacts, Patent WO2016184840A2, 2015
3. J.C.M. Choi, H. Park, Solar cell and method for manufacturing the same, Patent EP 2797124A1, 2013
4. D.L. Young, W. Nemeth, V. LaSalvia, R. Reedy, S. Essig, N. Bateman, P. Stradins, Interdigitated back passivated contact (IBPC) solar cells formed by ion implantation, IEEE J. Photovolt. **6**, 41 (2016)

5. F. Haase, C. Hollemann, S. Schäfer, A. Merkle, M. Rienäcker, J. Krügener, R. Brendel, R. Peibst, Laser contact openings for local poly-Si-metal contacts enabling 26.1%-efficient POLO-IBC solar cells, Solar Energy Mater. Solar Cells **186**, 184 (2018)
6. C. Reichel, R. Müller, F. Feldmann, A. Richter, M. Hermle, S.W. Glunz, Influence of the transition region between p- and n-type polycrystalline silicon passivating contacts on the performance of interdigitated back contact silicon solar cells, J. Appl. Phys. **122**, 184502 (2017)
7. C. Hollemann, F. Haase, M. Rienäcker, V. Barnscheidt, J. Krügener, N. Folchert, R. Brendel, S. Richter, S. Großer, E. Sauter, J. Hübner, M. Oestreich, R. Peibst, Separating the two polarities of the POLO contacts of an 26.1%-efficient IBC solar cell, Sci. Rep. **10**, 658 (2020)
8. R. Peibst, M. Rienäcker, Y. Larionova, N. Folchert, F. Haase, C. Hollemann, S. Wolter, J. Krügener, P. Bayerl, J. Bayer, M. Dzinnik, R. Haug, R. Brendel, Towards 28%-efficient Si single junction solar cells with better passivating POLO junctions, Sol. Energy Mat. Sol. Cells (submitted)
9. M. Rienäcker, Three-terminal tandem solar cellsenabled by back-contacted bottom cellsfeaturing passivating, carrier-selectivepolysilicon based junctions, Ph.D. dissertation, submitted to Gottfried Wilhelm Leibniz Universität Hannover, 2021
10. M.B. Hartenstein, S. Harvey, M. Page, D. Young, P. Stradins, S. Agarwal, Effect of dopant compensation on the conductivity of the intrinsic poly-Si isolation region in passivated ibc silicon solar cells, in *2020 47th IEEE Photovoltaic Specialists Conference (PVSC)*. IEEE (2020) pp. 2751–2753
11. K. Ramspeck, S. Reissenweber, J. Schmidt, K. Bothe, R. Brendel, Dynamic carrier lifetime imaging of silicon wafers using an infrared-camera-based approach, Appl. Phys. Lett. **93**, 102104 (2008)
12. M.K. Stodolny, J. Anker, C.J.J. Tool, M. Koppes, A.A. Mewe, P. Manshanden, M. Lenes, I.G. Romijn, Novel schemes of p+ poly-Si hydrogenation implemented in industrial 6 bifacial front-and-rear passivating contacts solar cells, in *35th European Photovoltaic Solar Energy Conference and Exhibition* (2018), pp. 414–417
13. A. Grove, D. Fitzgerald, Surface effects on pn junctions: Characteristics of surface space-charge regions under non-equilibrium conditions, Solid-State Electr. **9**, 783 (1966)
14. J.Y.W. Seto, The electrical properties of polycrystalline silicon films, J. Appl. Phys. **46**, 5247 (1975)
15. B. Tyagi, K. Sen, On the resistivity of polycrystalline silicon, Phys. Stat. Solidi **80**, 679 (1983)
16. C.H. Seager, Grain boundaries in polycrystalline silicon, Annu. Rev. Mater. Sci. **15**, 271 (1985)
17. H.N. Chern, C.L. Lee, T.F. Lei, An analytical model for the above-threshold characteristics of polysilicon thin-film transistors, IEEE Trans. Electr. Dev. **42**, 1240 (1995)
18. M.K.H. Mark Stewart, High performance gated lateral polysilicon PIN diodes, Solid-State Electr. **44**, 1613 (2000)
19. U. Römer, R. Peibst, T. Ohrdes, B. Lim, J. Krügener, T. Wietler, R. Brendel, Ion implantation for poly-Si passivated back-junction back-contacted solar cells, IEEE J. Photovolt **5**, 507 (2015)
20. M. Rienäcker, A. Merkle, U. Römer, H. Kohlenberg, J. Krügener, R. Brendel, R. Peibst, Recombination behavior of photolithography-free back junction back contact solar cells with carrier-selective polysilicon on oxide junctions for both polarities, Energy Proc. **92**, 412 (2016)
21. W. Olthuis, P. Bergveld, On the charge storage and decay mechanism in silicon dioxide electrets, IEEE Trans. Electr. Insulat. **27**, 691 (1992)
22. R.S. Bonilla, C. Reichel, M. Hermle, P. Hamer, P.R. Wilshaw, Long term stability of c-si surface passivation using corona charged SiO_2, Appl. Surf. Sci. **412**, 657 (2017)

Cite this article as: Michael Rienäcker, Yevgeniya Larionova, Jan Krügener, Sascha Wolter, Rolf Brendel, Robby Peibst, Rear side dielectrics on interdigitating p^+-(i)-n^+ back-contact solar cells − hydrogenation vs. charge effects, EPJ Photovoltaics **12**, 6 (2021)